Adaptive Motor Control to Aid Mobile Robot Trajectory Execution in the Presence of Changing System Parameters

Martin D. Adams, *Associate Member, IEEE*

***Abstract*—Most of the mobile robot path planning algorithms presented to date, generate intermediate goal coordinates for a mobile robot to pursue, based upon the local environment and the position of the global target. In response to this, we present a general controller for any vehicle which is driven by changing target vectors and show that the restricted speed (or torque) capabilities of the vehicle can be modeled with a nonlinear saturation element.**

Although the goal attraction path parameters can be optimized so that a vehicle tracks its target in a near time optimal sense, the effect of motor parameter changes or disturbances to the controlled system upon the path of the robot is noted. When the process gain of the robot's motors change, due to temperature changes, run-in time etc., we will show that the trajectory of the mobile robot is momentarily affected, before the closed loop control system again places the robot back on to its correct course.

In this article, a novel method is presented, which manipulates the effective nonlinear speed saturation element, which models the actual speed or torque limitations of any vehicle, in order to remove this problem. Simple modifications can be applied to the derived control system, so that mobile robot adaptive target tracking can take place. The conditions necessary, which can be exploited to allow the response of a mobile robot to be insensitive to changes in motoring parameters will be presented, and the method will be demonstrated by purposely inducing process gain changes on a real mobile robot.

***Index Terms*—Adaptive control, dual input describing function, limit cycle, mobile robot, parameter estimation, potential field, self-oscillating adaptive system, time optimal trajectory.**

I. Introduction

MANY of the mobile robot path planning algorithms presented in the literature, produce changing intermediate target coordinates for a mobile robot to pursue, based upon local sensor information and the position of the global target [1]–[4].

The control aspects of forcing a mobile robot to track changing target coordinates is therefore considered. In particular, the problem of changing motor parameters and their effect upon the trajectory of a mobile robot is addressed. A novel control adaptation technique is presented which is capable of removing unwanted path changes caused by motor process gain changes.

Manuscript received May 13, 1997; revised August 12, 1998. This paper was recommended for publication by Associate Editor W. R. Hamel and Editor V. Lumelsky upon evaluation of the reviewers' comments.

The author is with the European Semiconductor Equipment Centre (ESEC), Cham CH-6330, Switzerland.

Publisher Item Identifier S 1042-296X(98)08731-X.

It was shown in [5] that any real vehicle under the influence of a simple goal seeking algorithm will inherit a nonlinear control system. The general form of this control system is addressed in Section II.

In order to apply the general control algorithm to particular vehicles, an estimate of the system parameters or motor process gains is necessary. Section III shows that these parameters can vary with running time and temperature and can also be considered to vary due to system disturbances (changes in friction, system's mass etc.) and can ultimately cause a noticeable disturbance on the path of the mobile robot.

It appears that trajectory tracking errors which result from system parameter changes, have been noted in the literature regarding manipulator control, but seldom in any literature on mobile vehicle control. Adaptive robot trajectory control, using adaptive, robust controllers to compensate for the fact that a system's mass properties are, in general, not known *a-priori*, is a major current research issue [6]–[9]. In the work by Erlic and Lu [10] for example, an adaptive velocity observer was proposed for reducing the positional and velocity tracking errors of a Puma-560 robot manipulator. Tracking errors in the joint angles and speeds were recorded. An adaptive velocity observer was successfully implemented which was capable of reducing these errors, after a certain adaptation time.

In the mobile robot literature, errors in the path of an autonomous vehicle platform have been analyzed by Nelson and Cox [11], where the driven and steering angles of a three-dimensional (3-D) wheeled vehicle are controlled. It was noted that the errors in the steering angle of the mobile robot used, were more difficult to compensate than the errors in the distance driven. Achieving high gain error control, without causing an undesirable or even unstable response, required specialized pole-zero compensating filters, after which small errors in the robot's trajectory were still observed.

By analyzing a general, nonlinear, goal seeking controller using *describing functions*, Section IV demonstrates that the nonlinearity can cause limit cycle oscillations in the path of the mobile robot. The conditions to prevent such oscillations were examined in [5], [4] where it was further shown that targets could be reached time optimally by adjusting the gain of the nonlinearity.

The work is extended, by analyzing the undesirable trajectory changes caused by changing motoring parameters and by analyzing the possibility of using to advantage a small propagating limit cycle oscillation. It will be shown in Section

V that it is trivial to adjust the controller derived in [4] and shown in Section II, to produce a self-oscillating adaptive system (S.O.A.S.) [12] which automatically adapts to these undesirable parameter changes. It is capable of automatically changing the effective gain of the nonlinearity to input target signals in order to maintain a constant loop gain in the event of the process gain changing. The price paid for this form of adaptation is the presence of an oscillation, the amplitude, and frequency of which can change when the process gain changes. By ensuring that the amplitude of the allowed oscillation is small enough, the gear boxes on a mobile robot will be unable to respond to it, implying the possibility of an *adaptive* asymptotically stable system.

II. Non-Linear Mobile Robot Potential Attraction

In [4] and [5], it was shown that any real mobile robot which is controlled to track a target coordinate $\mathbf{x}$ based upon a desired coordinate $\mathbf{x}_d$, will automatically inherit a nonlinear control system, since the speeds (or torques) provided by its motors will, in reality, be restricted.

Koditschek [13] and Adams [4] considered the kinetic energy T and an imaginary potential energy ψ of a mobile robot, when operating under an artificial potential field algorithm, in order to derive a control algorithm. The kinetic energy is given by

$$T = \frac{1}{2} M \dot{\mathbf{x}}^T \dot{\mathbf{x}} \tag{1}$$

where M represents the total mass of the mobile robot and $\dot{\mathbf{x}}$ its velocity vector within the plane. To arrive at a linear control law, a quadratic Hooke's law function can be used for ψ as suggested by Volpe and Khosla [14]

$$\psi = \frac{1}{2} K_1 (\mathbf{x} - \mathbf{x}_d)^T (\mathbf{x} - \mathbf{x}_d) \tag{2}$$

where K_1 can be referred to as an attractive force constant.

All nonconservative (dissipative) forces $\mathbf{F}_{\text{ext}}$ which act on the mobile robot are given by the Lagrange equation [15], [16]

$$\frac{d}{dt}\left(\frac{\partial(T-\psi)}{\partial \dot{\mathbf{x}}}\right) - \frac{\partial(T-\psi)}{\partial \mathbf{x}} = \mathbf{F}_{\text{ext}} \tag{3}$$

which results in

$$\mathbf{F}_{\text{ext}} = M\ddot{\mathbf{x}} + K_1(\mathbf{x} - \mathbf{x}_d). \tag{4}$$

In (3), $\mathbf{F}_{\text{ext}}$ is by definition dissipative [16]. This can be implemented with a Rayleigh damping term

$$\mathbf{F}_{\text{ext}} = -K_2 \dot{\mathbf{x}} \tag{5}$$

the negative sign indicating *dissipation*, $\dot{\mathbf{x}}$ the velocity vector of the mobile robot and K_2 a positive dissipative force constant. By equating (5) with (4), applying the operator $s = \frac{\partial}{\partial t}$ and rearranging, the velocity of the robot can be determined as

$$\dot{\mathbf{x}} = \frac{K_1}{K_2}\left[\mathbf{x}_d - \left(1 + s^2 \frac{M}{K_1}\right)\mathbf{x}\right]. \tag{6}$$

Hence by considering the total energy of a mobile robot, when under the influence of an artificial potential field, it is possible to arrive at a control law, namely that the desired velocity signal to the motors should be dependent upon both position and *acceleration* feedback of the robot. This control law, along with the speed restriction of any real robot mentioned above, is implemented by the block diagram in Fig. 1.[1]

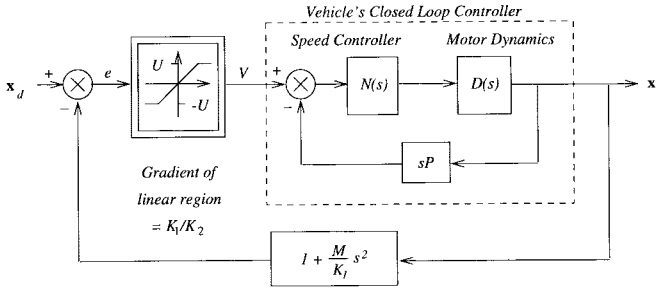

Fig. 1. A realistic control system for any vehicle with its own speed controller, under the influence of an artificial potential field.

In Fig. 1, the desired speed signal for the vehicle's closed loop controller is derived from the error signal between the actual and desired positions generated from the mobile robot's path planner. Note that the derived, desired speed signal V is restricted to $\pm U$ m/s to take into account the finite speed capabilities of the motors. $N(s)$ is the mobile robot's on board speed controller and $D(s)$ represents the vehicle's motor dynamics.

To ease the algebra, the vehicle's closed loop controller block in Fig. 1 can be represented as a single transfer function $H(s)$ where

$$H(s) = \frac{N(s)D(s)}{1 + sPN(s)D(s)} \tag{7}$$

$H(s)$ will be referred to as the process gain, since this contains the vehicle's controller and motoring parameters.

Before considering adaptive target tracking, two mobile robots which differ from each other greatly in their size and weight are introduced, along with an estimate of their motoring parameters.

III. Parameter Estimation

In the experimental analyses, the smaller of the two mobile robots was used. This robot (named Eric) weighs only 4.8 kg and was built using two permanent magnet d.c. motors [17], and is controlled by an *integral* speed controller (i.e. $N(s) = \frac{A}{s}$). Each motor takes a voltage signal which directly drives each wheel, hence translation of the mobile robot is related to the sum of the two signals and rotation is provided by the difference of the voltage levels applied to each motor. The second vehicle is tracked and was initially built for military purposes and weighs 62 kg. Again, it is driven by d.c. motors, but its speed controller is a *proportional* one (i.e., $N(s) = B$). Results of experiments using the first vehicle under the overall position control system in Fig. 1 will be demonstrated.

In order to analyze the response of each vehicle, a complete estimate of the robots' motoring parameters is necessary. A full

[1] For a mobile robot which controls the *torque* of its motors, the block diagram is similar and is explained in [4].

TABLE I
MOTORING PARAMETERS MEASURED AT VARIOUS TIMES AFTER THE MOTORS WERE FIRST SWITCHED ON. A SINGLE VALUE FOR EACH PARAMETER INDICATES THAT THE MEASURED PARAMETER WAS TIME INVARIANT. THE POSSIBLE OSCILLATION FREQUENCIES AND PROCESS (MOTOR) GAINS $H(j\omega_0)$ ARE ALSO SHOWN AT EACH TIME. K_T IS THE MOTOR TORQUE CONSTANT, M IS THE SYSTEM MASS, L THE ARMATURE INDUCTANCE, R_a THE ARMATURE RESISTANCE, C_F THE (ASSUMED LINEAR) RELATIONSHIP BETWEEN SPEED AND FRICTIONAL TORQUE, K_V IS THE MOTOR'S SPEED CONSTANT, AND P IS THE VELOCITY FEEDBACK GAIN (SEE FIG. 1)

Vehicle:		*ERIC*			*TRACKED VEHICLE*		
Motor Running Time (Seconds):		*3*	*60*	*180*	*3*	*60*	*180*
Parameter:							
K_V /(Vs/m)			42.308			26.74	
K_T /(Nm/A)			2.729			3.88	
C_F /(Ns)		0.041	0.037	0.032	48.5	40.74	31.04
R_a /(Ω)	low		11.4			0.3	
	high		12.5			0.6	
L /(mH)	low	1.093	1.094	1.047		42.0	
	high	1.165	1.155	1.160		90.0	
r /(m)			0.065			0.145	
M /(Kg)			4.78			62	
A /(s)			66.85			0	
B			0			3.8	
P /(Vs/m)			9.158			12.6	
U /(V)			2.5			5.0	
Osc Freq	low		20.74		18.42	18.34	18.24
ω_0/(rad/s)	high		21.72		27.65	27.44	27.16
Proc Gain	low 10e-3		2.78		2.59	2.76	2.99
$H(j\omega_0)$	high 10e-3		3.00		6.15	6.88	8.06

discussion on how this can be carried out is given in [4] and here, for brevity, the estimated parameters for each vehicle are given in Table I, where the parameters are explained in the caption.

The estimation of the motoring parameters for each of the vehicles tested have shown that changes in temperature (as a consequence of the running time for each vehicle) can slightly influence the process gain $|H(j\omega)|$, as indeed can a disturbance, such as a change in the robot's mass or the friction between its wheels and the surface upon which it maneuverers. A high gain in the speed controller accompanied by feedback should reduce the effects of changing parameters further. However a change in $|H(j\omega)|$ for one or both of the motors causes a sudden undesirable change in the output angular and Cartesian position of the robot as will be demonstrated in Section V. The closed loop system eventually removes the effect so that the mobile robot again positions itself on target, but an undesirable instantaneous response to any changes is still observable.

In control systems where parameter adaptation is crucial (for example in the pitch control of high speed aircraft), S.O.A.S. have been documented. [18], [19] explain two S.O.A.S. implementations for the pitch control of the X-15 aircraft, where large parametric changes occurred within the controlled process gain. This work demonstrates the effect of controlling

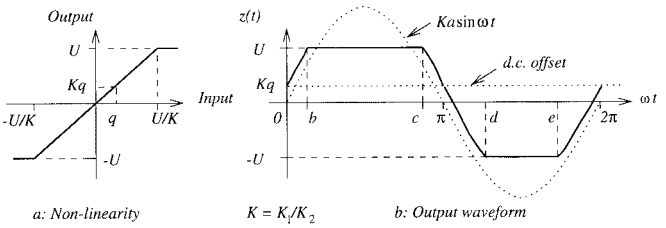

Fig. 2. Output waveform produced by the nonlinear saturation in response to the signal $w(t) = a\sin\omega t + q$ for $a > \frac{UK_2}{K_1} + q$. In the figure $K = K_1/K_2$.

either the amplitude or frequency of a propagating oscillation in order to allow parametric adaptation. The philosophy behind this technique is that provided the frequency is high enough, or the amplitude small enough, the pilot should be unable to detect the presence of the oscillation in the aircraft's pitch angle.

In [5], the aim was to analyze the derived control system of Fig. 1 to avoid any limit cycle in the mobile robot's motion. In this article, the backlash which is inherent in most gear boxes is used to advantage. It is possible to exploit an oscillation with an amplitude small enough to be unable to propagate through such a gear box so that the wheels of the mobile robot do not respond to it. It can also be arranged however, that the oscillation is able to propagate around the control loop to allow adaptation to take place.

IV. DESCRIBING FUNCTION ANALYSIS

It was noted in [5], that before any particular vehicle's controller or dynamics is considered, the nonlinear element in Fig. 1 can cause a limit cycle oscillation to propagate around the derived block diagram. This is demonstrated in Fig. 2, where the output waveform of the nonlinear element in response to an oscillatory input $a\sin\omega t$ and a slowly moving or "dc" input q caused by the error signal $\mathbf{x}_d - \mathbf{x}$ is considered. The complete input signal at the nonlinearity is defined as $\omega(t) = a\sin\omega t + q$.

To obtain an approximate transfer function for the nonlinear element, the *describing function* method can be applied to the system [20].

The output waveform can be represented as a Fourier Series

$$z(t) = N_0 + n_1\sin(\omega t + \phi) + n_2\sin(2\omega t + \phi) + n_3\sin(3\omega t + \phi) + \cdots \tag{8}$$

The signal $\mathbf{x}$ at the output of the linear motor dynamics will be the sum of these components, after each has been multiplied by $H(j\omega)$ (the transfer function of the vehicle's closed loop speed controller) in Fig. 1. In most real motor control systems, the harmonics of the signal $z(t)$ will be greatly attenuated by $H(j\omega)$. $z(t)$ is therefore approximated by its fundamental component only.

In Fig. 2(b), the values of b, c, d and e at the discontinuities in the output oscillation are given by

$$b = \sin^{-1}\left(\frac{U - Kq}{Ka}\right) = \sin^{-1}\theta$$
$$c = \pi - \sin^{-1}\left(\frac{U - Kq}{Ka}\right) \tag{9}$$

$$d = \pi + \sin^{-1}\left(\frac{U+Kq}{Ka}\right) = \pi + \sin^{-1} T\theta$$
$$e = 2\pi - \sin^{-1}\left(\frac{U+Kq}{Ka}\right) \tag{10}$$

where $K = \frac{K_1}{K_2}$ and $T = (U+Kq)/(U-Kq)$ and a new variable $\theta = (U-Kq)/Ka$ has been introduced to simplify the equations.

A. Self-Oscillating Adaptive Target Tracking

The principle behind a S.O.A.S. can be explained by considering the d.c. value N_0 in (8) of the output waveform in Fig. 2. This is given by

$$N_0 = \frac{1}{\pi}\left[a\cos\left(\sin^{-1}\left(\frac{U+Kq}{Ka}\right)\right) - a\cos\left(\sin^{-1}\left(\frac{U-Kq}{Ka}\right)\right) - (U-Kq)\left(\sin^{-1}\left(\frac{U-Kq}{Ka}\right)\right) + (U+Kq)\left(\sin^{-1}\left(\frac{U+Kq}{Ka}\right)\right)\right] \tag{11}$$

where Kq is the d.c. offset in the signal produced by the nonlinearity and a is the oscillation amplitude at entry to the nonlinearity. For large gradients $K = K_1/K_2$, the nonlinearity tends toward a perfect relay, so that

$$N_0 \approx \frac{2U}{\pi}\sin^{-1}\frac{q}{a}. \tag{12}$$

The *dual input describing function* $F'(a)$ represents the gain of the nonlinear element to "dc" or slowly changing signals and is defined as

$$F'(a) = \frac{\text{Amplitude of dc component of } z(t)}{\text{Amplitude of dc component of input}} = \frac{N_0}{q}. \tag{13}$$

For small values of q/a it can be seen from (12) that

$$F'(a) \approx \frac{2U}{\pi a}. \tag{14}$$

It can therefore be seen that the gain presented by the nonlinearity to slowly varying signals is dependent upon the amplitude a of the sinusoidal oscillation. Similarly, the describing function representing the transmission of the oscillation through the nonlinearity is defined as [20]

$$F(a) = Me^{j\phi} \tag{15}$$

where

$$M = \frac{\text{Amplitude of fundamental component of } z(t)}{\text{Amplitude of fundamental component of } w(t)} \tag{16}$$

and

$$\phi = \text{Phase angle by which fundamental of } z(t) \text{ leads fundamental of } w(t). \tag{17}$$

For large K_1/K_2, $F(a)$ is given by [4]

$$F(a) \approx \frac{4U}{\pi a} \tag{18}$$

so that the gain presented to the oscillation is approximately inversely proportional to the oscillation amplitude. If $G(j\omega)$ is defined as

$$G(j\omega) = H(j\omega)\left[1 + \frac{M}{K_1}(j\omega)^2\right] \tag{19}$$

then since $F(a)$ represents the transfer function of the nonlinearity to oscillations, it can be seen from Fig. 1, that when an oscillation occurs

$$|F(a)G(j\omega)| = 1 \tag{20}$$

meaning that the amplitude of the oscillation *automatically adjusts* so that the loop gain is unity at the frequency ω. Thus if the process gain $H(j\omega)$ and hence $G(j\omega)$ change with time, the oscillation amplitude will be forced to change such that (20) is still true. For the slowly varying signal (14) and (18) show that

$$F'(a) = \frac{1}{2}F(a). \tag{21}$$

This yields the possibility of turning the control system into a S.O.A.S. [21], the result of which can be described as follows. The nonlinearity acts as a variable gain to slow signals. The magnitude of this gain depends on the amplitude of the sinusoidal signal at the input to the nonlinearity. This gain is therefore automatically set by the limit cycle oscillation to such a value that the loop gain presented to reference signals, from (21), is 0.5 at the limit cycle frequency ω_0.

A problem now results. It has just been shown that provided a limit cycle oscillation is maintained within the control loop, the problem of a varying process gain to the desired input vectors $\mathbf{x}_d$ can be overcome. In [5] however, it was shown that in order for asymptotic stability, limit cycles at the output of the system must be avoided. Mathematically this meant that values for K_1 and K_2 had to be used to ensure that

$$\frac{-1}{F(a)_{\max}} < -|G(j\omega_0)| \tag{22}$$

where ω_0 is the frequency at which $\arg[G(j\omega)] = -180°$.

In the following section, a new method is proposed for combining the better qualities of both techniques in maintaining a stable limit cycle oscillation within the feedback cycle, *and* asymptotic stability at the output.

B. Artificial Production of the Feedback Signal

The method relies on the backlash which is inherent in most gear boxes and requires an oscillation small enough not to affect the wheel position (due to the backlash) but large enough to be measurable elsewhere within the system.

The direct source of the position estimate on board a mobile vehicle can take several forms (without the use of more elaborate localization algorithms [22], [23]) including the following.

1) For d.c. motors, as used on Eric and the tracked vehicle, it is possible to integrate an estimate of the back e.m.f. of each motor to provide the position vector $\mathbf{x}$ of the vehicle. If the back e.m.f. is electronically integrated with respect to time to yield a position estimate, drift inevitably occurs as the integrators will integrate the slightest voltage offsets between their amplifier inputs. Hence accurate position feedback for a mobile vehicle will, in practice, not be feasible using back e.m.f. estimates.
2) The motors themselves can have an encoder attached to their rotors so that any motion of each rotor is recorded, before backlash is encountered within the gear boxes.
3) An encoder measures the rotation of each wheel directly at the wheel, as is the case with Eric and the tracked vehicle.

Clearly of these methods, the most reliable position estimate results from the third technique, since only the motion of the vehicle is recorded rather than that of the motor shaft.

In inequality (22) there is a whole range of values for K_1 and K_2 capable of producing a large gradient K_1/K_2 and an oscillation at the input to the motors which has an amplitude small enough to be undetectable at the gear box output. It is an oscillation of this nature that needs to be exploited to produce an adaptive system. For undistorted propagation of this oscillation around the control loop in Fig. 1, a method for feeding back the actual position of the vehicle, with the signal $a\sin\omega_0 t$ superimposed upon it is needed. Initially this appears to be a disadvantage, since the third technique above, which provides by far the most accurate update of the vehicle's location, cannot be used in the feedback loop as the oscillation is not to be observable at the wheels. Instead of trading off accuracy in position for the sake of a propagating oscillation and hence an adaptive controller, a method which combines the advantages of both techniques now follows.

1) The back e.m.f. from each motor is integrated with respect to time to produce an estimate of the vehicle's position. This signal will reproduce most small stable oscillations superimposed upon a "crude d.c. estimate" of position.
2) Encoder measurements are taken directly from the wheels. These signals will vary relatively slowly, showing no oscillations if a is small enough.
3) The "d.c. signal" in 1 is removed from the integrated back e.m.f. signal and replaced with the better "d.c. estimate" produced in 2.
4) The new artificially produced signal is injected into the feedback element, ready for propagation around the system.

Fig. 3 shows the above scheme. The above method theoretically satisfies the requirements for no observable oscillations at the motor output, and allows the propagation of a stable oscillation around the control system.

It should be noted, that this method is applicable to any control system having the form of Fig. 1, provided at least two motoring outputs are available. It is then necessary that a certain range of oscillatory amplitudes exist which will be small enough for the actual output *not* to reproduce it, but large enough to be recorded faithfully at another output within the system.

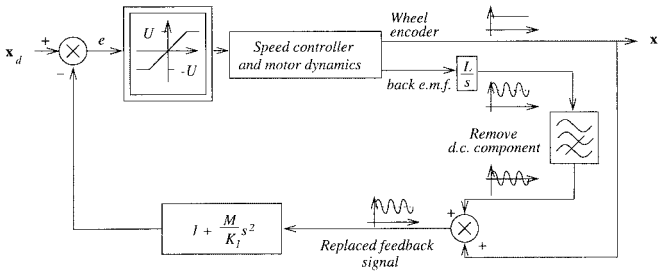

Fig. 3. Artificial production of the feedback signal allows the oscillation along with a reliable position estimate to propagate within the system.

V. Adaptive Target Tracking: Results

Before describing the experiments, it should be noted that if a high gradient (K_1/K_2) is used in the nonlinearity, and if the individual values of K_1 and K_2 violate inequality (22) then at oscillation, from (18), (20) in Section IV-A and the model of the motoring dynamics given in [4]

$$\frac{4U}{\pi a}\left(\frac{|(K_1(rMR_a+LC_F)-MAPK_T)|}{PK_1\sqrt{(R_aC_F+K_VK_T)^2+APK_T(rMR_a+LC_F)}}\right)=1. \tag{23}$$

This equation relates the oscillatory amplitude a to Eric's motoring parameters. [4] also shows that the oscillatory frequency ω_0 when

$$\arg[G(j\omega_0)]=-\pi \tag{24}$$

is given by

$$\omega_0=\sqrt{\frac{APK_T}{(rMR_a+LC_F)}}. \tag{25}$$

Using the parametric values from Table I the result obtained from (23) is

$$a\approx\left|0.009-\frac{19.809}{K_1}\right| \tag{26}$$

provided $K_1a/K_2 \gg U$.

A simple experiment was carried out in which new targets were injected into Eric's control system at times $t=0$, $t=3$ and $t=8$ s in order to examine the response of the vehicle. At time $t=4.5$ s, the process gain of one of the motors was purposely reduced by almost a factor of two in order to exaggerate the effect of changes in the motor gains. At time $t=6.5$ s the gain of the other motor was also decreased by a factor of two. This change was brought about by increasing the time constants, $(1/A)$, of the integral controllers by almost a factor of two, thus changing the process gains $|G(j\omega_0)|$. Note that if A is reduced from its initial value of $A\approx 67$ s^{-1} to $A\approx 35$ s^{-1}, (23) then gives the oscillation amplitude as

$$a\approx\left|0.010-\frac{32.270}{K_1}\right|. \tag{27}$$

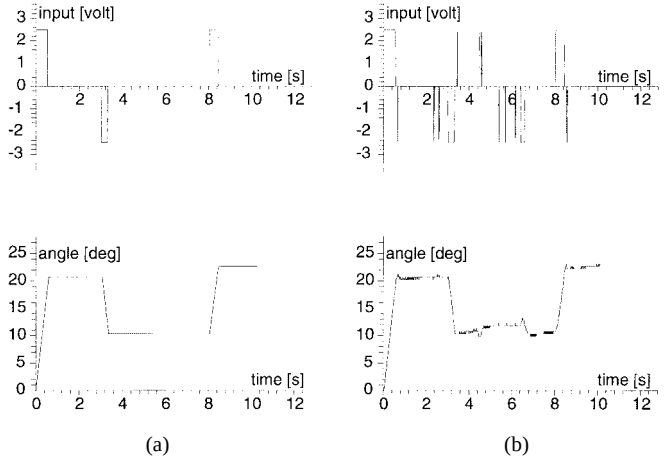

Fig. 4. Input speed curves and angular output curves for Eric. The left hand curves show a theoretically perfect bang bang control system response. The right hand graphs show the actual response with constants set to $K_1 = 20$ and $K_2 = 0.01$ in order to obtain no oscillations. At times $t = 4.5$ and $t = 6.5$ s the process gain of each motor was halved. Notice that the vehicle momentarily responds to the changes and in each case moves off course.

The left hand graphs in Fig. 4 show the variation of the differential input voltage supplied to the motors and the output angle with time that would be expected with a perfect system, unaffected by process gain changes. When the difference in the voltages applied to each motor reaches zero in the top left hand graph, the mobile robot is facing its target and then proceeds in a straight line to it.

The right hand graphs show the actual response when $K_1 = 20.0$ and $K_2 = 0.01$ obeying inequality (22) for no oscillations (Note: the fully derived form of inequality (22) in terms of K_1 and K_2 is given in [4]). The graphs show that the mobile robot is forced off target by each change. The overall closed loop system is able to adjust to the angular position of the vehicle such that it is once again on target. The path of the vehicle is affected for about 0.5 s in each case, as it recovers from an unwanted 3° rotation from its course.

The graphs shown in Fig. 5 show the results of the same experiment as above but this time values of K_1 and K_2 were chosen in order to produce a stable oscillation. The gains were once again reduced at times $t = 4.5$ s and $t = 6.5$ s. Note the rapid adaptation as the oscillation amplitude is reduced at $t = 6.5$ s, as predicted by (26) and (27). It can be seen from the graphs that at both times, when each process gain is changed, the mean value of the oscillatory signal does not appear to deviate at all from the required pursuit angle, as the nonlinearity is forced to automatically change its gain to the slowly varying signals by the change in oscillation amplitude [see (14)]. This result is required *without* the oscillation at the wheels.

It is during a mobile robot's straight line motion only that an oscillation in its angular position can propagate, and hence parameter adaptation can take place. This is because of the earlier assumption leading to (14), that $a \gg q$. It can be seen in the graphs (Figs. 4–8), that adaptation can only occur when very small or no changes in the desired steering angle q are input to the steering controller.

The graphs in Figs. 4 and 5 show the typical response of

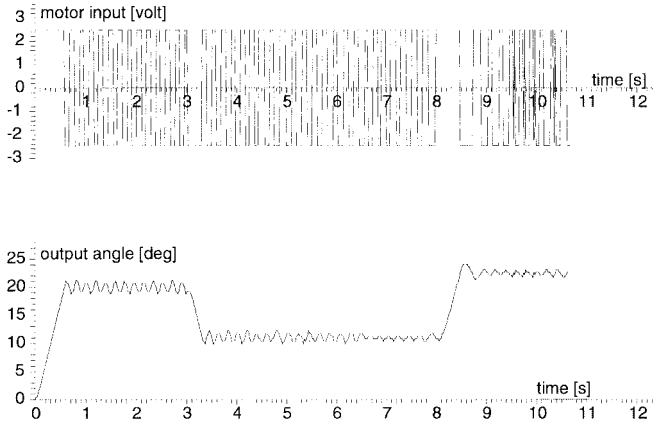

Fig. 5. Input angular speed signal and output angle when $K_1 = 6600$ and $K_2 = 0.5$ chosen in order to observe oscillations. At times $t = 4.5$ and $t = 6.5$ s the process gains were again halved. Note the rapid adaptation.

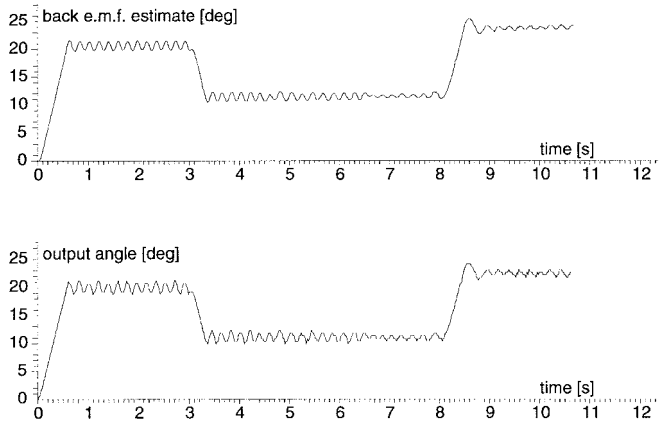

Fig. 6. Output angle versus time as estimated by integrating the difference in the motor back e.m.f.s (top graph) and estimated by the wheel shaft encoders when forced to oscillate. (This lower graph is repeated from the lower graph in Fig. 5 for comparison with the back e.m.f. estimate).

the mobile robot to the step change inputs (injection of new target vectors $\mathbf{x}_d$) shown in the top left hand graph of Fig. 4. It can be seen that under this simple form of control, the mobile robot spends only a small fraction of its time rotating and most of its time moving in a straight line toward its target.

The top graph in Fig. 6 shows the output angle of the mobile robot as estimated by electronically integrating the difference in the back e.m.f.s from each motor. The lower graph shows the actual output angle as measured by the odometers versus time. Note that the oscillation is much more sinusoidal in its appearance since sampling from the odometers is no longer relied upon to reconstruct it. It must also be noted however, that the d.c. level of the signal (or output angular estimate) can slowly drift with time, due to small unavoidable voltage offsets within the operational amplifier integrator.[2]

Experiments were conducted to determine the maximum amplitude of an oscillation which could be seen from the integrated difference in the back e.m.f.s of each motor, but

[2] An automatic gain control system was therefore used to reduce this effect in the experiments.

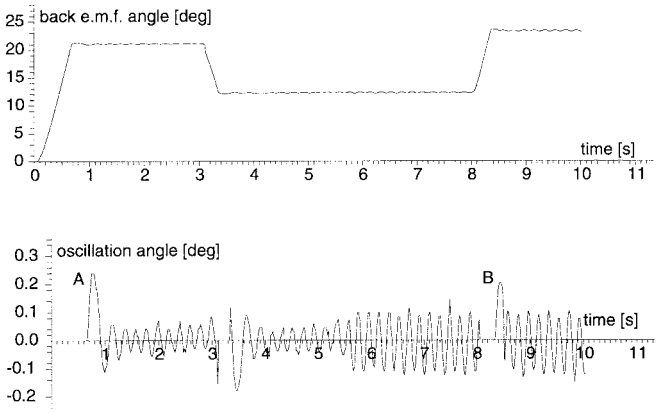

Fig. 7. The back e.m.f. angular estimate under the artificially created adaptive controller. The bottom graph shows the oscillatory component only. The values of K_1 and K_2 used to obtain these results were $K_1 = 3000.0$ and $K_2 = 0.5$ as explained in the text.

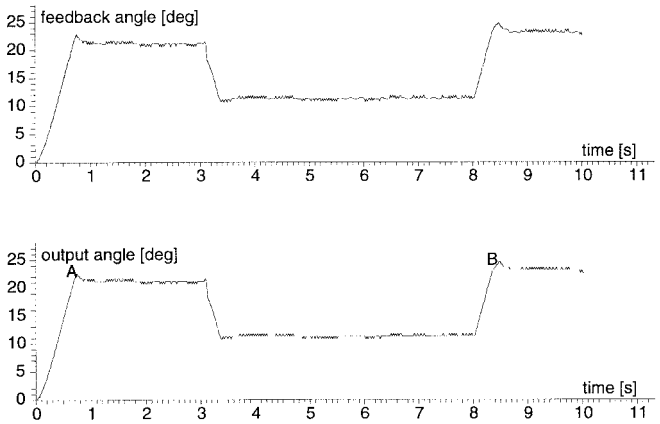

Fig. 8. The fabricated signal ready for input into the feedback element (top graph) and the resulting output angle of the vehicle assensed by the odometers (bottom graph). Note that no deviation in angle when the process gains change can be observed.

could not be observed at the output (the robot's wheels). The maximum permissible amplitude for Eric's crude odometric system was found to be 0.72° of rotation, which would correspond to a wheel displacement of almost 0.003 meters at the point of contact between the wheel and the floor.

In Fig. 7, the integrated back e.m.f. difference is shown along with just the oscillation (all slowly varying signals removed) versus time, as the mobile robot pursues different targets at times $t = 0$, $t = 3$ and $t = 8$ s, as before. In this experiment the gains of both motor controllers were doubled from $A \approx 35$ s^{-1} to $A \approx 70$ s^{-1} at $t = 5.2$ s simultaneously. A value for K_1 was chosen in order to produce an oscillation with an amplitude of approximately 0.001 meters when $A \approx 35$ s^{-1} at $q = 0$, using (26). To produce an amplitude $a = 0.001$ m, the attractive force constant necessary is $K_1 \approx 3000$. To implement the control strategy of Fig. 3, any signals with frequency lower than ω_0 must be removed. The remaining oscillation frequencies, from the integrated difference in the back e.m.f.s, are then added onto the odometric output. This new signal is then ready for propagation around the system. Note the increase in amplitude by approximately a factor of two at time $t = 5.2$ s and the corresponding increase in frequency by approximately a factor of $\sqrt{2}$ in the bottom graph of Fig. 7 [see (25)]. The top graph in Fig. 8 shows the angular estimate produced from the odometers and the oscillation added together. Note that the oscillation cannot be observed at the wheels since the sawtooth waveform caused by the odometers in the top graph is larger than the amplitude of the small oscillation present. This signal is fed to the feedback element. Finally the bottom graph in Fig. 8 shows the output angle measured from the wheel encoders. Note that the sawtooth waveform with amplitude approx 0.5° in the output angle curves is not an oscillation but results from the discretized angular space caused by the odometry. After angular convergence, the wheels rotate at the same speed thus causing no overall further change in the angle of the vehicle. The linear position of the vehicle is however still changing, and if the odometers on each wheel detect motion out of phase with each other, the sawtooth waveform results. The desired result has been achieved as no oscillations and no change in the angle, the angle can be observed, when the process gains are changed.

Erlic and Lu reported in their work, manipulator joint angle tracking errors, noted as a result of system parameter disturbances, of 1° in joint angle position and 4°/s in joint velocity. An adaptive velocity observer was able to reduce these errors to less than 0.3° and 0.3°/s, respectively, after an adaptation time of approximately 5 s [10].

One advantage that can be noted in this work, is that although adaptation is paid for in the form of a change in amplitude and frequency of a propagating oscillation, the adaptation itself is immediate, as the system requires no time for parameter estimation as in other adaptive systems [7], [9].

VI. Overshoot in the Nonlinear System

Careful inspection of the previous output angle curves will reveal that small overshoots occur as the new angles are reached. This is particularly noticeable at points A and B in the graphs of Figs. 7 and 8. In a nonlinear system there is no general method for analyzing overshoot, and the describing function method used offers an oscillatory analysis only.

Past simulation studies of S.O.A.S. systems by Horowitz [24] and Gelb [25], [19] have shown that system response to signals not satisfying the initial assumptions (that q/a is small and that q varies more slowly than $a \sin \omega_0 t$) is very sensitive to the limit cycle phase at the instant of application of the signal q. The response can vary between extreme overshoot and undershoot [24].

In the system described here, the application of the new step target vector $\mathbf{x}_d$ forces the system to respond to an oscillation $a \sin \omega_0 t$ and a transient signal q which, for an instant in time (when the overshoot is observed), does *not* vary more slowly than $a \sin \omega_0 t$.

The describing function analysis in Section IV-A becomes a more accurate representation of the nonlinearity, when the desired signal $\mathbf{x}_d$ suddenly changes, if ω_0 is increased. This can be seen in the graphs in Figs. 6 and 7. When the oscillation has a higher frequency, the overshoot is reduced.

By changing A, the integral speed controller's time constant (Note that $N(s) = \frac{A}{s}$ for Eric), it was possible to change ω_0 [see (25)] and it was possible to change the amount of overshoot observed, as shown in Figs. 6 and 7. Unfortunately, changing the parameters in (25) so that ω_0 is increased can also increase the oscillation amplitude a, making it large enough to be observable at the wheels. Keeping a small enough and ω as large as possible reduced the observed overshoots when new angular targets were reached, but it was not possible in practice to remove overshoot altogether.

VII. Conclusion

It has been shown that adjusting a goal seeking control algorithm so that it automatically adapts to motor parameter changes can be a simple task.

Motoring parameters are difficult to estimate as it was shown that they can change as the motors run. Modifying the control system derived in [5] and shown in Section II so that it can adapt to changes of motor gains is trivial. A novel approach has been demonstrated which is very effective at removing the problems caused by process gain changes, with the minimum of change to the control system. The overall gain of the system to the input target vectors $\mathbf{x}_d$ is held constant, even if the process gain changes, without any noticeable loss in positional accuracy and without any adaptation time requirements.

A fair criticism is that, the poorer qualities of a nonideal gear box, in the form of backlash, is used to advantage. Most real vehicles however rely on reduction gear boxes, which means that any small oscillation at the motor shaft would often not be observable at the wheels.

To carry out the experimental analysis in this section, changes in the process gain were purposely induced on a real mobile robot. This was done to exaggerate the effect of motor parameter changes. It would be interesting to apply the method to larger vehicles, where the effect of parameter variations may be much more noticeable.

Acknowledgment

The author would like to thank P. J. Probert, SERC, for supporting this work.

References

[1] V. J. Lumelsky and A. A. Stepanov, "Path-planning strategies for a point mobile automaton moving amidst unknown obstacles of arbitrary shape," *Algorithmica*, vol. 2, pp. 403–430, 1987.
[2] R. A. Brooks, "Solving the find-path problem by good representation of free space," *IEEE Trans. Syst. Man Cybern.*, vol. SMCA-13, pp. 190–197, 1983.
[3] G. Giralt, R. Chatila, and M. Vaisset, "An integrated navigation and motion control system for autonomous multisensory mobile robots," in *Proc. 1st Int. Symp. Robot. Res.*, 1982, p. 191.
[4] M. D. Adams, "Optical range data analysis for stable target pursuit in mobile robotics," Ph.D. dissertation, Univ. Oxford, U.K., 1992.
[5] M. D. Adams and P. J. Probert, "Mobile robot motion planning—Stability, convergence and control," in *Proc. Int. Conf. Intell. Robots Syst.*, 1991, pp. 1019–1024.
[6] J.-J. E. Slotine and W. Li, *Applied Nonlinear Control*. Englewood Cliffs, NJ: Prentice-Hall, 1991.
[7] R. H. Middleton and G. C. Goodwin, *Digital Control and Estimation, A Unified Approach*. Englewood Cliffs, NJ: Prentice-Hall, 1990.
[8] L. L. Whitcomb, S. Arimoto, T. Naniwa, and F. Ozaki, "Adaptive model-based hybrid control of geometrically constrained robot arms," *IEEE J. Robot. Automat.*, vol. 13, pp. 105–116, Feb. 1997.
[9] K. Kaneko and R. Horowitz, "Repetitive and adaptive control of robot manipulators with velocity estimation," *IEEE J. Robot. Automat.*, vol. 13, pp. 204–217, Apr. 1997.
[10] M. Erlic and W. S. Lu, "A reduced-order adaptive velocity observer for manipulator control," in *IEEE J. Robot. Automat.*, vol. 9, pp. 328–333, 1993.
[11] W. L. Nelson and I. J. Cox, "Local path control for an autonomous vehicle," in *Proc. IEEE Int. Conf. Robot. Automat.*, 1988, pp. 1504–1510.
[12] K. J. Astrom and B. Wittenmark, *Computer Controlled Systems*. Englewood Cliffs, NJ: Prentice-Hall, 1987.
[13] D. E. Koditschek, *Robot Planning and Control Via Potential Functions—From the Robotics Review*. Cambridge, MA: M.I.T Press, 1989.
[14] P. Khosla and R. Volpe, "Superquadric artificial potentials for obstacle avoidance and approach," in *Proceedings of the IEEE International Conference on Robotics and Automation*, Philadelphia, PA, April 26–28, 1988.
[15] R. Weinstock, *Calculus of Variations*. New York: Dover, 1974.
[16] H. Goldstein, *Classical Mechanics*. Reading, MA: Addison-Wesley, 8th ed., 1971.
[17] M. D. Adams, "A mobile robot platform," Tech. Rep., Robot. Res. Group, Oxford Univ., U.K., 1988.
[18] M. O. Thompson and J. R. Welsh, "Flight test experience with adaptive control systems," in *Proc. Agard Conf. Adv. Contr. Syst. Concepts*, 1970, vol. 58, pp. 141–147.
[19] A. Gelb, "The analysis and design of limit cycling adaptive automatic control systems," Ph.D. dissertation, Mass. Inst. Technol., Cambridge, 1961.
[20] O. L. R. Jacobs, *Introduction to Control Theory*. Oxford, U.K.: Clarendon, , 1974.
[21] K. J. Astrom and B. Wittenmark, *Adaptive Control*. Reading, MA: Addison-Wesley, 1988.
[22] R. Hinkel and M. Weidmann, "First results in real time position estimation with a laser radar," Tech. Rep., Comp. Sci. Dept., Univ. Kaiserslautern, Germany, 1989.
[23] J. Leonard and H. F. Durrant-Whyte, "Navigation by correlating geometric sensor data," Tech. Rep. OUEL 1788/89, Robot. Res. Group, Oxford Univ., U.K., 1989.
[24] I. M. Horowitz, "Comparison of linear feedback systems with self-oscillating adaptive systems," *IEEE Trans. Automat. Contr.*, vol. 9, pp. 386–392, 1964.
[25] A. Gelb and W. E. V. Velde, "On limit cycling control systems," in *IEEE Trans. Automat. Contr.*, vol. 8, pp. 142–157, 1963.

Martin D. Adams (S'90–A'96) received the B.S. degree in engineering science and the D.Phil. degree from the University of Oxford, Oxford, U.K., in 1988 and 1992, respectively.

He became a Post Doctoral Research Assistant at the Institute of Robotics, Swiss Federal Institute of Technology, Zurich, Switzerland from 1992 to 1996. From 1994 to 1995, he was a Guest Professor with the NTB, Buchs, Switzerland, teaching control theory. Since September 1996, he has been a Research Scientist in robotics and control at the European Semiconductor Centre, Cham, Switzerland. His interests include adaptive control, mobile robot navigation, sensor design, and data interpretation.